Long-Range Corrected DFT Calculations of First Hyperpolarizabilities and Excitation Energies of Metal Alkynyl Complexes

Mahesh S. Kodikara, Rob Stranger* and Mark G. Humphrey

Abstract: The performance of the CAM-B3LYP, ωB97X and LC-BLYP long-range corrected density functional theory methods in the calculation of molecular first hyperpolarizabilities (β) and low-lying charge transfer (CT) excitation energies of the metal alkynyl complexes M(C≡C-4-C_6H_4-1-NO_2)(κ^2-dppe)(η^5-C_5H_5) [M = Fe (**1**), Ru (**2**), Os (**3**)] and *trans*-[Ru{C≡C-(1,4-C_6H_4C≡C)$_n$-4-C_6H_4-1-NO_2}Cl(κ^2-dppm)$_2$] [*n* = 0 (**4**), 1 (**5**), 2 (**6**)] was assessed. The BLYP, B3LYP and PBE0 standard exchange-correlation functionals and the Hartree–Fock method were also examined. The BLYP functional was shown to perform poorly in the calculation of β and low-energy CT transitions. The hybrid functionals (B3LYP and PBE0) showed significant improvement over the pure functional BLYP, but overestimated the hyperpolarizability ratios and the wavelengths of the lowest energy metal-to-ligand CT transitions for **5** and **6**. The effect of long-range corrections is noteworthy, particularly for the larger complexes, improving the calculation of β ratios for **4**–**6**. However, CAM-B3LYP, ωB97X, and LC-BLYP considerably overestimated the low-lying CT energies. PBE0 was found to give the best transition energy match for **4**. The influence of the phenylene ring orientation in the alkynyl ligand on the calculated properties is substantial, particularly for the larger complexes. For these types of calculations, a basis set with diffuse functions (at least 6-31+G(d)) for the heavy elements is recommended.

1. Introduction

Interest in highly efficient nonlinear optical (NLO) materials has grown enormously over the past two decades. This is mainly due to their potential in many applications such as optical computing, optical communications, optical switches, and optical storage.[1–5] Various systems have been investigated in recent years for their NLO activity. In particular, coordination and organometallic complexes have attracted significant attention because they expand the possibilities for tuning NLO properties by varying the metal center (and its oxidation state and co-ligands) when compared to organic chromophores.[6–10] Metallocenyl and metal alkynyl complexes are the two most scrutinized classes of NLO-active organometallic complexes, with the latter being found to exhibit record values of nonlinear optical coefficients.[11–13]

Quantum chemical calculations play a very important role in understanding structure–property relationships. When reliable, these calculations avoid performing unnecessary laboratory experiments and also guide the experimentalist in designing chromophores with optimal nonlinear activity.[14–17] An accurate computational model is usually selected by a critical comparison of different methods.[18–22] In such benchmark studies involving small molecules, the NLO data generated by coupled cluster theory is usually used to benchmark other methods.[21,23–25] The Møller–Plesset second-order perturbation theory has also been found to yield reasonably accurate NLO data.[18,21,26,27] Hyperpolarizabilities are significantly affected by electron correlation,[28] but such post-Hartree-Fock calculations are computationally intractable for larger molecules such as organometallics. As a result, density functional theory (DFT) methods have been routinely used to predict the NLO coefficients of larger chromophores due to a favorable accuracy/cost ratio, but the reliability of standard DFT functionals for these types of calculations has been questioned in the literature.[18,29–31] In response to these criticisms, the recent development of long-range corrected (LRC) DFT methods has been shown to reduce the errors associated with conventional XC functionals.[20,32–36]

Electric field-induced second-harmonic generation[37] (EFISH) and hyper-Rayleigh scattering[38,39] (HRS) are two experimental techniques that have been widely used to determine molecular first hyperpolarizabilities β. HRS measurements are relatively easy to perform compared to EFISH and can be applied to a broader range of chromophores, including octupolar[40,41] and ionic compounds.[42,43] In contrast, EFISH requires a knowledge of the third-order polarizability γ and the dipole moment μ to extract β, and is inapplicable for ionic species and nonpolar molecules.[44–46] For the past decade, HRS has been the method of choice in determining the quadratic hyperpolarizabilities of metal alkynyl complexes.[17,47–49]

Despite the large number of studies reporting DFT/time-dependent DFT (TD-DFT) linear optical and nonlinear optical calculations, critical comparisons of the different DFT functionals that have been employed in the calculation of the low-lying charge-transfer (CT) excitation energies and second-order polarizabilities β of large organometallic complexes are sparse. In an earlier paper,[50] we reported the first hyperpolarizabilities and linear optical properties of selected metal alkynyl complexes using the BP86, SAOP, and GRACLB DFT functionals (ADF program) and found that SAOP and GRACLB lead to static first hyperpolarizabilities that were comparable to the values obtained from BP86. In addition, preliminary calculations

[*] M. S. Kodikara, Em. Prof. R. Stranger, Prof. M. G. Humphrey
Research School of Chemistry, Australian National University
Canberra, ACT 2601 (Australia)
E-mail: Rob.Stranger@anu.edu.au

Supporting information for this article is given via a link at the end of the document.

employing the range-separated (RS) functionals CAM-B3LYP and LC-BLYP revealed a significant influence on the magnitude of β and afforded much better hyperpolarizability ratios compared to those obtained using analogous functionals lacking long-range corrections (B3LYP and BYLP).

The strong influence of long-range corrections on the calculated properties encouraged us to further investigate the performance of these functionals with regard to not only first hyperpolarizability calculations (both static and dynamic at 1064 nm) but also low-lying CT transitions of the metal alkynyls, which are usually related to their NLO-activity.[6] In the present work, we have calculated the first hyperpolarizabilities and low-lying CT transitions for the metal alkynyl complexes shown in Figure 1 employing the CAM-B3LYP, ωB97X, and LC-BLYP LRC-DFT functionals. The conventional DFT functionals BLYP, B3LYP, and PBE0, along with the Hartree-Fock (HF) method, have also been examined. The complexes **1**–**6** represent a range of donor-bridge-acceptor metal alkynyl complexes for which experimental data are available (see Table 1).

Three LRC-DFT functionals (LC-BLYP, CAM-B3LYP, and ωB97X) were employed. The LC-BLYP functional combines GGA-BLYP and the long-range correction proposed by Likura et al.[51] In this LRC scheme, the Coulomb operator, $1/r_{12}$, for the exchange functional splits into short-range (SR) and long-range (LR) parts with the help of the standard error function as follows:

$$\frac{1}{r_{12}} = \frac{1 - erf(\mu r_{12})}{r_{12}} + \frac{erf(\mu r_{12})}{r_{12}} \qquad (1)$$

The range separation parameter μ determines the ratio of these parts. In this approach, the DFT exchange functional (i.e. a slightly modified version) is used for the SR part and the HF exchange integral for the LR part, leading to the correct $-1/r$ asymptotic behavior in the long-range region. In LC-BLYP, for the SR part,

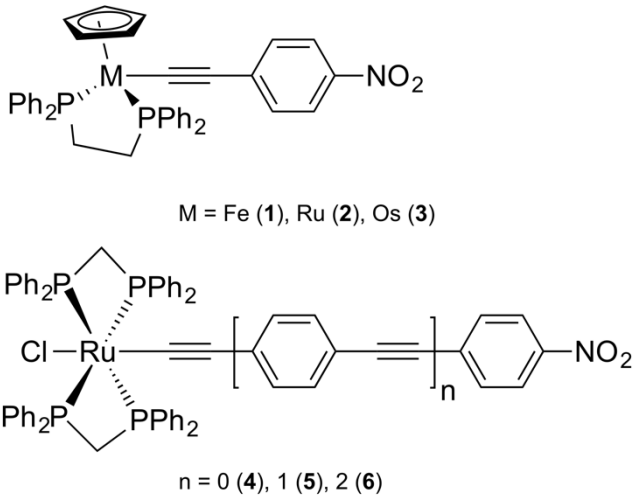

Figure 1. Metal alkynyl complexes used in this study

Table 1. Summary of the experimental linear optical and nonlinear optical data of **1**–**6**.

Complex	λ_{max}[a]	β_{HRS}[b]	β_{TLM}[c]	Ref.
1	498	665	64	[52]
2	447	664	161	[52]
3	461	929	188	[52]
4	473	767	129	[53]
5	464	833	161	[54]
6	439	1379	365	[54]

[a] Lowest-energy absorption maximum in THF. Values in nm. [b] Hyper-Rayleigh scattering measurements in THF at 1064 nm. Values in 10^{-30} esu. Errors±10% [c] Two-level corrected data. [55,56] $\beta_{TLM} = \beta_{HRS}[1 - (2\lambda_{max}/1064)^2][1 - (\lambda_{max}/1064)^2]$. Values in 10^{-30} esu.

the B88 exchange functional is employed and the LYP correlation functional is combined with the LRC exchange functional. The GGA-BLYP functional is the non-LRC version of LC-BLYP. B3LYP and PBE0 are two hybrid functionals containing 20% and 25% HF exchange, respectively, and have incorrect ($-0.2/r$ in B3LYP and $-0.25/r$ in PBE0) asymptotic behavior at LR. Applying the Coulomb-attenuating method (CAM) to the global hybrid B3LYP functional, Handy and co-workers[35] introduced a LRC-DFT functional known as CAM-B3LYP. In this approach, the two-electron operator (Eq. 1) is modified by introducing two extra parameters α and β as follows:

$$\frac{1}{r_{12}} = \frac{1 - [\alpha + \beta . erf(\mu r_{12})]}{r_{12}} + \frac{\alpha + \beta . erf(\mu r_{12})}{r_{12}} \qquad (2)$$

α and (α+β) describe the fraction of the exact exchange at r_{12}= 0 and $r_{12} = \infty$, respectively. When α = 0.0 and β = 1.0, this approach is equivalent to the above LC scheme of Likura et al. In CAM-B3LYP, the B88 exchange functional is employed, HF exchange is incorporated according to Eq. 2, and 0.19 VWN5+0.81 LYP is used as the correlation segment. We used the default values for α (0.19) and β (0.46), with $\mu = 0.33$. However, the CAM-B3LYP model does not have correct–$1/r$ asymptotic behavior at LR as the fraction of HF exchange at LR is less than 1. For our third RS functional, we used ωB97X from Gordon and co-workers,[36] which corresponds to the LR version of the exchange-correlation functional B97. ωB97X contains 100% HF exchange at LR and 16% short-range HF exchange, thereby leading to correct $-1/r$ asymptotic behavior (or no self-interaction errors) at LR. Details regarding these schemes can be found in Refs.[35,36,57], while Refs.[32,58–64] contain related work. A summary of the DFT functionals chosen for this study is provided in Table 2.

Computational Studies

All calculations were performed using the Gaussian09 program suite.[65] Full geometries of **1**–**3** without any symmetry constraints and of **4**–**6** with C_{2V} symmetry constraints were optimized using the Becke[66] three-parameter exchange Lee-

Yang-Parr[67] correlation functional (B3LYP). This functional is known to give

Table 2. Summary of DFT methods examined in this study for the determination of the first hyperpolarizabilities and excitation energies of **1**–**6**, and the amount of exact-exchange at short-range, SR, and long-range, LR.

Method	Type	%HF exchange		Range-separation parameter μ (au^{-1})
		SR	LR	
BLYP[67,68]	GGA	0	0	[a]
B3LYP[66,69]	Hybrid	20	20	[a]
PBE0[70]	Hybrid	25	25	[a]
CAM-B3LYP[35]	Range-separated	19	65	0.33
ωB97X [36]	Range-separated	15.8	100	0.30
LC-BLYP[57]	Range-separated	0	100	0.33

[a] Not applicable

reasonably accurate geometries for transition metal complexes.[71] The 6-31G(d) basis set was used for the ligands, whereas for Fe/Ru/Os, the pseudo potentials of Stuttgart/Dresden and associated SDD basis sets were utilized.[72] Solvent corrections were found to have only a minor influence on the bond distances and angles (see Table S1). Thus, for the rest of the study, the geometries optimized *in vacuo* were used. However, solvent corrections were found to be important for the evaluation of the first hyperpolarizabilities (see Table S2).

The first hyperpolarizability tensors were calculated analytically in the static limit ($\lambda = \infty$) and at 1064 nm (experimental wavelength). Using the resulting components, the β^0_{calc} (static β) and β^{1064}_{calc} (dynamic β at 1064 nm) quantities were calculated (see supporting information for more details). The calculated values were obtained using the B convention. As such, to compare with the experimental data, the Gaussian-derived β values were divided by a factor of two. The percentage contribution of groups of atoms to the selected molecular orbitals were obtained using the GaussSum3.0[73] program. Solvent corrections were taken into account by means of the implicit CPCM solvation model in tetrahydrofuran (THF) during the β and UV-Vis calculations. The 6-311G(d,p) basis set for the ligands and SDD basis set for the transition metals were used in the property calculations unless otherwise stated.

2. Results and Discussion

2.1. First hyperpolarizabilities β

Static β. The calculated static first hyperpolarizabilities β^0_{calc} of complexes **1**–**6** are reported in Table 3 along with the experimental two-level corrected data (β_{TLM}). In these systems, β_{zzz} greatly dominates over the other elements, as expected for dipolar complexes, consequently, Eq. 5 (see supporting information) was used to calculate the first hyperpolarizabilities. For instance, in the case of complex **5**, for all methods used, the β_{calc} value derived for the dominant β_{zzz} element decreased between 0-4% when all elements were considered in the calculations.

The calculated static first hyperpolarizabilities β^0_{calc} for all complexes decrease significantly upon incorporating the long-range correction. For example, in the case of **1**–**4**, an order of magnitude decrease in β^0_{calc} is seen when the corrections are incorporated in BLYP (LC-BLYP vs BLYP). The impact is amplified with an increase in molecular size. The β^0_{calc} of **6** using LC-BLYP decreases by nearly two orders of magnitude compared to that of BLYP. These predictions suggest that β decreases with increasing amount of HF exchange (i.e. LR HF exchange) in the functional. Overall, the general hyperpolarizability trend as a function of method is invariant for all the complexes: BLYP > B3LYP > PBE0 > CAM-B3LYP > ωB97X > LC-BLYP > HF.

The two-level derived hyperpolarizability data were used as a reference (see Table 1) despite the known inadequacy of this simple model for many molecular systems.[74–76] The two-level derived value of 64×10^{-30} esu for **1** is underestimated by the RS functionals, whereas the conventional methods, including hybrid functionals, overestimate the value. Clearly, the discrepancy is method-dependent (Table 3). For **2**-**4**, all the functionals underestimate the respective β_{TLM} values (**2**, 161×10^{-30} esu; **3**, 188×10^{-30} esu; **4**, 129×10^{-30} esu). The β^0_{calc} values of **5** and **6** using BLYP appear to be unrealistically large when compared to the two-level data (**5**, 161×10^{-30} esu; **6**, 365×10^{-30} esu). B3LYP and PBE0 significantly improve the estimate of hyperpolarizabilities but still overestimate their values. All the RS functionals and the HF method underestimate the β_{TLM}. The ability to calculate accurate absolute hyperpolarizability data, however, is rarely important; the ability to predict reliable trends in the NLO data is more important for designing efficient NLO materials.

One common approach for enhancing β is extending the conjugation (e.g. **4** to **5** and **5** to **6**). The two-level corrected hyperpolarizability ratios between **4**–**6**, A = $\beta_{TLM,\mathbf{5}}/\beta_{TLM,\mathbf{4}}$ and B = $\beta_{TLM,\mathbf{6}}/\beta_{TLM,\mathbf{4}}$, are approximately 1.2 and 2.8, respectively. The performance of the LRC-DFT and HF methods (A = 2.5 and B = 2.8 for CAM-B3LYP; A = 2.0 and B = 2.2 for ωB97X; A = 1.9 and B = 2.1 for LC-BLYP; A = 2.2 and B = 2.6 for HF) is much better than that of the conventional functionals (A = 11.4 and B = 48.2 for BLYP; A = 5.3 and B = 7.8 for B3LYP; A = 4.4 and B = 6.1 for PBE0). The worst predictions of A and B are shown by BLYP. These predictions are consistent with our previous study.[50] Except for BLYP, all the DFT methods reproduce the two-level corrected trend for **1**–**3** (i.e. **1** < **2** < **3**), and no functional predicts the significant difference between the two-level corrected values of **1** and **2** (Table 3).

Frequency-Dependent β. Calculations are often reported in the static limit. In contrast, the experimental data is usually obtained at a certain laser frequency (e.g. at 1064 nm in this case). Consequently, frequency-dependent β values at 1064 nm were calculated for **4**–**6**. The C_{2v} symmetry of these complexes significantly reduces the computational demand for the calculation of frequency-dependent β values compared to

complexes **1**–**3** which have no symmetry. The resulting calculated dynamic hyperpolarizabilities (β_{calc}^{1064}) for **4**–**6** are given in Table 3.

It should be noted that the experimental hyper-Rayleigh scattering data of **4**–**6** at 1064 nm is likely to be resonance enhanced, similar to most of the data for group 8 metal alkynyl complexes reported to date.[48,52–54,77] Consequently, attention is focussed on the relative β responses upon increasing the conjugation (i.e. **4** < **5** < **6**).

The RS functionals have successfully reproduced the HRS trend (**4** < **5** < **6**) and are free from the resonance effects in the calculated data because the low-energy transitions modelled by the RS functionals are considerably removed from the second-harmonic signal at 532 nm (discussed later). In contrast, the BLYP dynamic β for **4**–**6** are significantly resonance enhanced, in particular, the β_{calc}^{1064} data of **5** and **6**. For example, the TD-DFT-

Table 3. Calculated first hyperpolarizabilities with a variety of DFT functionals and with the HF method. Values in 10^{-30} esu.

Complex	BLYP	B3LYP	PBE0	CAM-B3LYP	ωB97X	LC-BLYP	HF	Exp.
				β_{calc}^{0} ($\lambda = \infty$)				β_{TLM}
1	129.7	87.6	74.5	40.2	27.5	23.3	12.2	64
2	112.2	92.9	81.7	51.1	35.4	30.0	19.8	161
3	111.5	102.5	91.7	61.7	43.1	37.5	26.3	188
4	117.7	92.0	80.4	49.2	34.0	28.6	17.5	129
5	1344.1	487.0	354.3	121.0	68.2	54.8	39.2	161
6	5675.6	721.3	486.8	138.7	76.2	60.4	45.6	365
				β_{calc}^{1064} (λ = 1064 nm)				β_{HRS}
4	231.2	1094.3	370.2	93.9	50.5	39.4	21.4	767
5	69135.3	1521.6	2342.6	355.2	132.7	96.5	63.2	833
6	10902.7	2450.0	2695.7	439.3	162.4	115.9	81.9	1379

BLYP data obtained for **5** indicate two intense transitions that are very close in energy to the fundamental and second-harmonic wavelengths. The resonance effects have a more profound impact on the β_{calc}^{1064} values of **5** and **6** by PBE0 than on those obtained with B3LYP, leading to an unexpected trend for the B3LYP and PBE0 values (i.e. B3LYP < PBE0 for **5** and **6**). Both hybrid functionals reproduce the relative trends, as do the RS functionals.

Conformational Effect. In previous work, we underlined the importance of considering the effect of conformational flexibility on the β values, particularly for the larger complexes (e.g. **5** and **6** in the present study), because β decreases sharply when the geometry deviates from the ideal coplanar arrangement; the poor performance shown by BLYP might partly be attributed to ignoring this factor in the preceding hyperpolarizability calculations.

To assess the impact of conformational flexibility, one- and two-dimensional scans of the potential energy surfaces (PESs) of **2** and **5** were calculated, respectively. Figure 2 shows the scan variables while the resulting energy surfaces are given in the supporting information (Figure S2). From the PESs, the energies required to rotate the alkynyl ligands of **2** and **5** with respect to the metal center, or to change the relative orientations of the phenylene groups in the alkynyl ligand of **5**, are very small. Thus, under laboratory conditions, a mixture of conformations is expected to co-exist in equilibrium. To investigate conformational effects, β_{calc}^{0} was evaluated for selected points on the potential energy surfaces of **2** and **5**, the resulting data being provided in Table 4. The general trend does not appear to be affected by the geometry of the complex. For instance, for any rotamer of **2** and **5**, β_{calc}^{0} decreases in the order BLYP > B3LYP > PBE0 > CAM-B3LYP > ωB97X > LC-BLYP > HF. For the RS and hybrid DFT functionals, a variation of 30-35% in calculated β values was predicted for **2** upon increasing θ, while the variation is less than 15% for BLYP. The two-level corrected data of **2** (161×10^{-30} esu) is larger than the calculated values in Table 5 for all the DFT functionals and the HF method. The influence of the aryl orientation on the β_{calc}^{0} value is more profound in the case of **5** than for **2** mainly due to the effect of the second scan variable ϕ which defines the relative orientation between two phenylene groups in the alkynyl ligand.

Upon increasing ϕ from 0° to 90° (while maintaining θ at 0°), the electronic communication between the donor and acceptor groups is adversely affected, leading to a significant reduction in the β_{calc}^{0} values. However, BLYP shows an increase in the β_{calc}^{0} value when ϕ changes from 0° to 45°, the reason for which is not clear. For **5**, the RS functionals show a variation of more than 60% of the computed data between the maximum and minimum values, while the variation is more than 80% for the conventional methods. These large variations indicate the strong sensitivity of the calculated β value to the initial molecular geometry, irrespective of the method chosen, and this is particularly marked for the larger complexes. The values from the RS methods and the HF method for **5** (Table 4) are less than the respective two-level corrected data, which, however, lie in the range (between the maxima and minima) computed by the conventional methods.

Overall, conformational effects cannot be ignored for these complexes, especially for the larger molecules. Although not practical, a thorough investigation of the conformational space is required before one can properly compare the DFT calculations

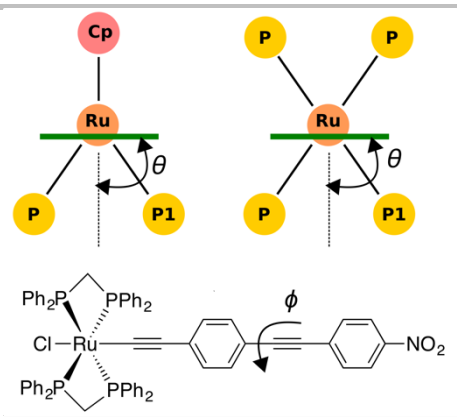

Figure 2. Variables used in the potential energy scans of **2** and **5**. θ defines the rotation of the aryl ring with respect to the metal centre, while ϕ is the second scan variable of **5** and defines the relative orientations of the two aryl groups in the alkynyl ligand. The resulting energy surfaces and further details are given in the supporting information.

Table 4. Calculated static first hyperpolarizabilities (β^0_{calc}) for selected conformations of **2** and **5**. Values in 10^{-30} esu.[a]

Conformation	BLYP	B3LYP	PBE0	CAM-B3LYP	ωB97X	LC-BLYP	HF	Exp.
θ				**2**				β_{TLM}
0	111.7	95.4	84.4	53.4	37.0	31.4	20.7	161
45	111.8	85.7	74.6	45.5	31.5	26.7	18.0	
90	98.1	65.6	56.7	34.7	24.5	20.9	14.8	
135	108.8	80.5	69.9	42.4	29.6	25.0	17.0	
180	110.4	93.4	82.4	51.8	35.8	30.4	20.0	
(θ,ϕ)				**5**				
(0, 0)	1344.1	487.0	354.3	121.0	68.2	54.8	39.2	161
(45, 0)	1314.8	419.1	310.2	108.9	62.6	50.8	37.9	
(0, 45)	1540.2	326.5	229.1	77.1	46.3	37.6	26.9	
(45, 45)	1493.3	298.7	211.6	73.0	44.0	36.0	26.3	
(90, 0)	1048.9	372.2	280.8	103.8	60.1	49.4	37.5	
(0, 90)	120.2	60.2	53.5	34.4	26.3	22.0	15.0	
(90, 90)	205.1	53.3	47.3	31.1	24.0	20.3	14.6	

[a] θ ≈ –20° is for the fully optimized structure of **2** (Table 3). θ ≈ 0° and ϕ = 0° are for the (C_{2v}) coplanar rotamer of **5** (Table 3).

with the experimental data. However, it is important to note that calculations on the coplanar rotamers reproduce the experimental and two-level hyperpolarizability trends. The relative β values computed in this study for coplanar and noncoplanar rotamers of **5** are consistent with our previous data.[50]

Basis Set Effect. Choice of basis set is crucial in the calculation of field response properties; extended basis sets usually being required.[14,26,78–80] Complexes **2** and **4** were selected to investigate the basis set influence on β^0_{calc}. Figure 3 shows the β^0_{calc} values of **2** and **4** as a function of the basis set used for the heavy elements with the indicated DFT functional. The numerical values are given in Table S3.The basis set effects on the larger complexes **5** and **6** are expected to be smaller, as a result of some superposition effect.[14,21,81,82] Five split basis sets were chosen: two polarized basis sets, 6-31G(d,p) and 6-311G(d,p), with no diffuse s and p functions, and three basis sets with diffuse functions, 6-31+G(d,p), 6-311+G(d,p), and 6-311++G(d,p). In addition, the 6-31+G(d) basis set was also considered. In all cases, the SDD basis set on the metal was retained as earlier work as shown that basis set effects are less important for the central metal compared to the surrounding ligands.[50]

As shown in Figure 3, the diffuse functions have a profound effect on the calculated hyperpolarizability. For example, the β^0_{calc} values increase by 35 – 40% for **2** and **4** with the addition of a set of diffuse functions to 6-31G(d,p), i.e. 6-31+G(d,p). Apparently, convergence is achieved with the 6-31+G(d). Hence, it is important to use diffuse functions for the ligands (at least the 6-31+G(d) basis set) in any quantitative analysis. However, there is little effect on β from adding a set of valence functions (e.g. 6-31G(d,p) vs 6-311G(d,p)) as well as augmenting the 6-31+G(d) and 6-311+G(d,p) basis sets with polarization functions for hydrogens and heavy elements. Note that diffuse functions have no influence on the general trend in DFT performance, i.e. BLYP > PBE0 > LC-BLYP. Further, the β^0_{calc} values are much more sensitive to the method (e.g. BLYP vs LC-BLYP) than whether or not the basis set contains diffuse functions.

The 6-31+G(d) basis set has been used In numerous studies[21,22,26] for the determination of β, as a trade-off between accuracy and efficiency. In Table S4, the β^0_{calc} values for **1**–**6** with 6-31G(d,p), 6-311G(d,p), and 6-311+G(d,p) are provided. On the basis of the data in this table, it is clear that the relative hyperpolarizability trend for **1**–**6** is unaffected by diffuse functions.

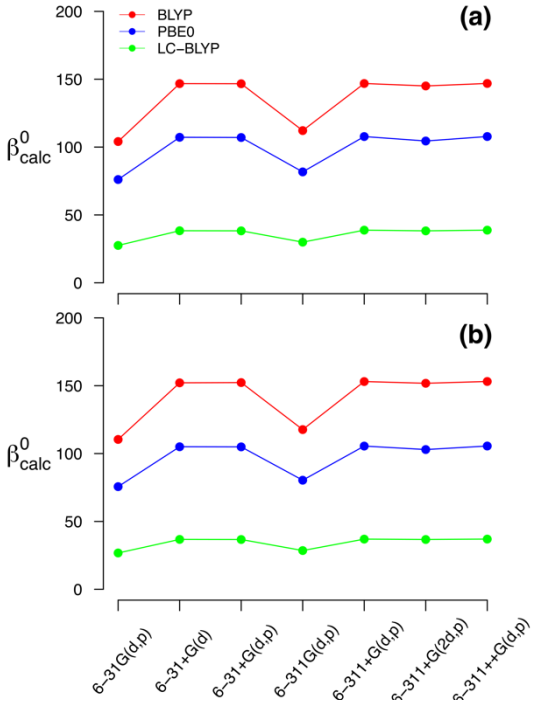

Figure 3. The static hyperpolarizabilities (10^{-30} esu) of **2 (a)** and **4 (b)** as a function of the basis set used for the heavy elements. Pseudopotentials of Stuttgart/Dresden and the associated SDD basis set for Ru were employed.

2.2. Excitation Energies

In this section, the performance of BLYP, B3LYP, PBE0, CAM-B3LYP, ωB97X, and LC-BLYP functionals in calculating excitation energies of the metal alkynyl complexes has been assessed. The calculated data, i.e. vertical excitation energies and corresponding oscillator strengths, are summarized in Tables 5-7 for **2**, **4**, and **5**, respectively, together with the major orbital pairs that contribute to the excited-state wavefunctions. The contribution of groups of atoms to the relevant molecular orbitals of **2**, **4**, and **5** are provided in Tables S5-S7, respectively. The relevant experimental UV-Vis absorption maxima have been used for comparison. The calculated results are summarized below.

The GGA functional BLYP significantly underestimates the excitation energies for **2**. Two intense excitations at 626 nm and 566 nm were obtained from BLYP, with the former being considerably more intense. The BLYP lowest-energy transition, resulting from a HOMO to LUMO excitation, is predominantly metal-to-ligand charge transfer (MLCT) in character (see Table 5 and S5) and is considerably red-shifted with respect to the experimental absorption maximum of 447 nm.

Incorporating a constant amount of HF exchange into the pure functional (i.e. hybrid DFT) greatly improves the result, in agreement with an earlier study.[22] The B3LYP (20% HF) functional yields two excitations at 531 nm and 493 nm. The PBE0 functional (25% HF) outperforms B3LYP, yielding two excitations at 492 nm and 455 nm. The HOMO to LUMO excitations computed from the hybrid functionals show similar MLCT character. When LRC is incorporated, both excitation energy and oscillator strength increase dramatically for the HOMO to LUMO transition. A sharp increase in the HOMO-LUMO gap with the introduction of LRC accounts for the increase in the excitation energy found for the RS functionals, as shown in Table S8. Note that the low-lying transitions are significantly blue-shifted with respect to the experimental low-energy band for the LRC-DFT methods, particularly for the ωB97X and LC-BLYP functionals.

The compositions of the HOMO and LUMO are somewhat different for BLYP and its LRC analogue (LC-BLYP), the contribution of the [C≡CC_6H_4] group increasing for the latter. This may explain the discrepancies in the oscillator strengths obtained for the two functionals. The HF excitation energy is quite inaccurate for the HOMO to LUMO transition, being even higher than the LC-BLYP-calculated energy. Overall, the TD-DFT studies show that the PBE0 and CAM-B3LYP functionals outperform the other DFT functionals in the calculation of the excitation energy of the low-lying MLCT band.

For **4**, BLYP predicts one intense transition in the low-energy region (< 400 nm), which is red-shifted by approximately 160 nm compared to the experimental band at 473 nm (Table 6). Again, the two hybrid functionals significantly improve the calculated band position; in fact, PBE0 outperforms all other functionals (see Table 6). In comparison with our previous data,[50] there is excellent agreement. The RS functionals overestimate the excitation energy, as found for **2**, with the shift from the experimental data being method-dependent. The energy associated with the HOMO to LUMO transition essentially increases with the amount of LR HF exchange in the functional and correlates with the HOMO-LUMO gaps (Table S8). This intense transition is MLCT in character for all the functionals (see Table 6 and S6).

According to Table 7, the lowest-energy band for **5** calculated by BLYP appears in the NIR region (1030 nm). This is a significant underestimation of the CT energy corresponding to the lowest-energy peak at 464 nm in the experimental UV-Vis but is comparable to our previous TD-DFT results predicted for **5**.[50] Similarly, the hybrid functionals also overestimate the excitation energies, but the absolute errors are much smaller. The lowest energy band results from the HOMO to LUMO excitation for all the standard functionals, thus indicating the MLCT character of this transition (Table S7). In contrast, the same bands predicted using the RS functionals consist of several single excitations between different molecular orbitals (Table 8), but show significant MLCT character. CAM-B3LYP, ωB97X and LC-BLYP all overestimate the excitation energy for this band. As found for **2** and **4**, the shift from the experimental wavelength of 464 nm is method-dependent. For all three complexes, the HF method yields poor excitation energies which significantly overestimate the experimental band. Note that the reported experimental values are reduced to a single wavelength–absorption maximum. This makes the comparison with the calculated data difficult, particularly when two or more transitions with non-negligible oscillator strength are predicted in the absorption region. In general, the calculated vertical excitation energies will not correspond to the maximum

absorption, owing to the vibronic nature of the transitions and the change of geometry upon excitation.

For the metal alkynyl complexes, the low-energy MLCT transitions dictate their β responses.[6] The energy of the Intense, lowest-energy transition in **2**, **4**, and **5** increases significantly when long-range corrections are incorporated and therefore the static β calculated from the RS-DFT methods are significantly smaller than those derived from conventional functionals for these complexes, according to the two-level model.[55,56]

Bridge Length Effect. Although it seems counterintuitive that extending the conjugation, on proceeding from **4** to **5**, results in a blue-shift in the lowest-energy MLCT band, this is not uncommon for dipolar metal alkynyl complexes containing oligo(phenyleneethynylene) π-bridges.[83–86] According to the experimental UV-Vis data, further extending the conjugation from **5** to **6** leads to a blue-shift in the lowest energy CT band (Table 1). Previous studies[87,88] for similar species have suggested that the observed blue-shift in the absorption maximum is due to the internal rotation of the phenylene groups about the C(ipso)-C≡ bonds in solution. Studies on related systems[89] have shown that the TD-DFT calculations on a single conformer fail to explain the absorption band envelopes. This unexpected blue-shift in the intense, low-energy MLCT band was also reported upon increasing the conjugation length by Yam et al.[90] for polyyne metal complexes. These authors have suggested that the blue-shift arises due to the greater stabilization of the dπ orbital with increasing C≡C chain length.

In this section, we extended our TD-DFT calculations to investigate the effectiveness of these functionals in predicting the experimental data upon increasing the bridge length from 4 to 5 to 6. The excited state properties computed for the first four (singlet) excited states of **4**–**6** are given in Table 8 for BLYP, B3LYP, and their LRC versions (for results with the remaining functionals, see Table S9). Note that all calculations were performed on the C_{2v}-symmetric coplanar conformations of **4**–**6**, i.e. for **5** and **6** the aryl rings in the alkynyl ligand are coplanar and in the plane bisecting the dppm ligands.

On the basis of the TD-BLYP data given in Table 8, the A_1 excitation that arises from the HOMO to LUMO transition is substantially red-shifted as the conjugation increases from **4** to **5** to **6**. The two hybrid functionals also afford a red-shift in the lowest energy excitation. Conventional functionals thus fail to reproduce the blue-shift observed experimentally following bridge lengthening. A recent study by Sahnoune et al.[91] has suggested that long-range corrections are needed to reproduce the experimentally observed blue-shift in the absorption maxima upon proceeding from n = 0 to n = 2 in the series Fe{C≡C-(1,4-C_6H_4C≡C)$_n$-4-C_6H_4-1-NO_2}(κ^2-dppe)(η^5-C_5H_5). However, in our case, CAM-B3LYP predicts a red-shifted HOMO to LUMO excitation (proceeding from **4** to **5**), similar to the prediction with the conventional functionals, but upon further extension of the π-conjugation, the RS version of B3LYP yields a slight blue-shift of ca. 7 nm. This is, however, much less than the laboratory blue-shift of ca. 25 nm (on proceeding **5** to **6**). Moreover, several single excitations contribute to the first (S_1) excited-state wavefunction, although the HOMO to LUMO excitation still makes the largest contribution. No such blue-shift in the intense A_1 transition is predicted with the ωB97X and LC-BLYP functionals. Note that the energetic order of the electronic transitions differs between the standard functionals and their LRC versions. For example, for **4**, the first four transitions are to A_2, A_1, B_2, and B_1 states (Table 9) for TD-BLYP. On the other hand, the LC-BLYP data shows that the order is B_2, B_1, A_2, and A_1. Overall, all the functionals fail to reproduce the laboratory blue-shift observed for **4**-**6**.

Table 5. Calculated wavelengths (λ) and corresponding oscillator strengths (f) for **2** employing the listed DFT functional. Only the first 12 excited states with f < 0.1 are included.

Method	λ (nm)	[f]	Major contribution
BLYP	626	0.402	HOMO → LUMO
	566	0.120	HOMO–2 → LUMO
B3LYP	531	0.350	HOMO → LUMO
	493	0.293	HOMO–1 →LUMO
PBE0	492	0.473	HOMO → LUMO
	455	0.227	HOMO–1 → LUMO
CAM-B3LYP	400	0.808	HOMO → LUMO
ωB97X	362[a]	0.147	HOMO → LUMO+1
	354	0.767	HOMO → LUMO
LC-BLYP	337	0.873	HOMO → LUMO
HF	316[a]	0.248	HOMO → LUMO
	308	0.715	HOMO → LUMO
Exp.	447		

[a] Several single excitations between different molecular orbitals were found. Only the orbital pair giving the largest contribution is reported.

Table 6. Calculated wavelengths (λ) and corresponding oscillator strengths [f] for **4** employing the listed DFT functional. Only the first 12 excited states with f < 0.1 are included.

Method	λ (nm)	[f]	Major contribution
BLYP	632	0.533	HOMO → LUMO
B3LYP	511	0.645	HOMO → LUMO
PBE0	479	0.670	HOMO → LUMO
CAM-B3LYP	397	0.830	HOMO →LUMO
ωB97X	355	0.890	HOMO → LUMO
LC-BLYP	337	0.900	HOMO → LUMO
HF	309	0.863	HOMO → LUMO
Exp.	473		

Table 7. Calculated wavelengths (λ) and corresponding oscillator strengths [*f*] for **5** employing the listed DFT functional. Only the first 12 excited states with f < 0.1 are included.

Method	λ (nm)	[f]	Major contribution
BLYP	1026	0.616	HOMO → LUMO

	546	0.289	HOMO–3 → LUMO
	500	0.636	HOMO → LUMO+2
B3LYP	664	0.767	HOMO → LUMO
	406	1.014	HOMO–3 → LUMO
PBE0	598	0.892	HOMO → LUMO
	379	1.084	HOMO → LUMO+1
CAM-B3LYP	415	1.695	HOMO → LUMO
	292[a]	0.461	HOMO–2 → LUMO
ωB97X	363[b]	2.013	HOMO → LUMO
LC-BLYP	346[b]	2.016	HOMO → LUMO
HF	336[b]	1.905	HOMO → LUMO
Exp.	464		

[a] Several single excitations between different molecular orbitals were found. Only the orbital pair giving the largest contribution is reported. [b] HOMO to LUMO contribution is ca. 50%, which is considerably lower than that obtained with BLYP, B3LYP, PBE0, and CAM-B3LYP functionals (> 70%).

Conformational Effect. Intramolecular rotations usually have significant impact on the UV-Vis behavior of these complexes.[50] In the preceding section, we showed that the conformational effects on β are substantial, particularly for the larger complexes. This in turn made the comparison between functionals difficult to evaluate. In this section, we extend our TD-DFT calculations to investigate the influence of phenylene group(s) orientation in the π-bridge on the low-lying UV-Vis data. For several rotamers of **2** and **5**, the first 15 states were calculated using the BLYP, PBE0, CAM-B3LYP, and LC-BLYP functionals. Stick spectra of the oscillator strengths for **2** and **5** are shown in Figures S3 and S4, respectively. The low-lying linear optical behavior of **2** and **5** are significantly affected by the intramolecular rotations, defined by the θ and ϕ dihedral angles (Figure S1), as shown by Figures S3 and S4, respectively. Further, owing to the small energy barriers associated with these rotations, the experimental UV-Vis profiles

Table 8. Calculated excitation energies (λ, nm) and oscillator strengths [f] of the first four lowest-energy (singlet) transitions of **4**–**6** with a variety of DFT functionals.

Method	Transition	Symm.	λ (nm)	[f]	Symm.	λ (nm)	[f]	Symm.	λ (nm)	[f]
			4			**5**			**6**	
BLYP	S_1	A_2	739	[0.000]	A_1	1026	[0.616]	A_1	1492	[0.419]
	S_2	A_1	632	[0.533]	A_2	1006	[0.000]	A_2	1205	[0.000]
	S_3	B_2	526	[0.002]	B_1	638	[0.000]	B_1	709	[0.000]
	S_4	B_1	523	[0.000]	B_2	552	[0.003]	A_1	666	[1.061]
B3LYP	S_1	A_2	527	[0.000]	A_1	664	[0.767]	A_1	723	[0.555]
	S_2	A_1	512	[0.645]	A_2	567	[0.000]	A_2	573	[0.000]
	S_3	B_2	441	[0.002]	B_2	457	[0.003]	A_1	477	[1.674]
	S_4	B_1	428	[0.000]	B_1	444	[0.000]	B_2	461	[0.003]
CAM-B3LYP	S_1	A_1	397	[0.830]	A_1	415	[1.695]	A_1	409	[2.747]
	S_2	B_2	397	[0.001]	B_2	405	[0.002]	B_2	406	[0.002]
	S_3	B_1	384	[0.000]	B_1	392	[0.000]	B_1	393	[0.000]
	S_4	A_2	374	[0.000]	B_1	355	[0.002]	B_1	355	[0.002]
LC-BLYP	S_1	B_2	379	[0.001]	B_2	385	[0.001]	B_2	385	[0.001]
	S_2	B_1	368	[0.001]	B_1	374	[0.000]	B_1	375	[0.000]
	S_3	A_2	348	[0.000]	A_2	349	[0.000]	A_1	350	[3.125]
	S_4	A_1	337	[0.900]	A_1	346	[2.016]	A_2	349	[0.000]

of **2** and **5** presumably results from the overlap of individual bands of many conformers. The intensities of the low-lying transitions in **2** change noticeably upon increase in θ. For BLYP, PBE0, and CAM-B3LYP, the relative intensities of the (higher-energy) neighbouring transitions to the HOMO-to-LUMO transition were found to increase with increasing θ from 0° to 90° (Figure S3). The experimental absorption maximum of **2** is at 447 nm. BLYP overestimates this for all the rotamers, while LC-BLYP significantly underestimates the absorption maximum. Compared to CAM-B3LYP, the PBE0 performance improves after incorporating conformational effects.

With **5**, the intensities of the low-lying transitions diminish significantly as ϕ increases; when ϕ = 90°, no intense transitions appear in the region above 400 nm for all the methods (Figure S4). From Figure S4, it seems that these internal rotations do not entirely account for the underestimated excitation energy calculated by BLYP and PBE0 for the lowest-energy MLCT band, whereas the transition energy is overestimated by CAM-B3LYP and LC-BLYP.

Basis Set Effect. In this section, we have examined the effects of basis set on the excitation energies. Complex **4** was selected as a test case. The HOMO to LUMO excitation was calculated with BLYP, PBE0, and LC-BLYP using the 6-31G(d,p), 6-31+G(d), 6-31+G(d,p), 6-311G(d,p), 6-311+G(d,p), 6-311+G(2d,p), and 6-311++G(d,p) basis sets. Pseudopotentials of Stuttgart/Dresden and the associated SDD basis set for Ru were used in all cases. The resulting data are presented in Table 9.

From Table 9, the excitation energy (λ_{max}) of the intense, lowest-energy transition is seen to converge as the basis set is augmented beyond 6-31+G(d); further augmentation has a minor effect. Adding diffuse functions to the second- and third-row elements has a considerable impact, but the shift is functional-dependent. For example, for BLYP the displacement

of λ_{max} from6-31G(d,p) to 6-31+G(d,p) is ca. 50 nm, while it is only ca. 20 nm in the case of LC-BLYP. Adding an extra set of valence functions, from 6-31G(d,p) to 6-311G(d,p), has a moderate impact

Table 9. Basis set effect on the HOMO-to-LUMO transition in **4** computed using BLYP, PBE0, and LC-BLYP functionals.

Basis set	BLYP	PBE0	LC-BLYP
	λ (nm) [f]	λ (nm) [f]	λ (nm) [f]
6-31G(d,p)	619 [0.54]	471 [0.69]	330 [0.91]
6-31+G(d)	672 [0.60]	508 [0.71]	352 [0.93]
6-31+G(d,p)	673 [0.59]	508 [0.71]	352 [0.93]
6-311G(d,p)	632 [0.53]	479 [0.69]	337 [0.90]
6-311+G(d,p)	674 [0.59]	509 [0.70]	353 [0.92]
6-311+G(2d,p)	669 [0.60]	505 [0.71]	352 [0.93]
6-311++G(d,p)	674 [0.61]	509 [0.70]	353 [0.92]

on the excitation energy. The PBE0/6-31G(d,p) level of theory was found to give the best match with the experimental absorption maximum at 473 nm. The general trend in the calculated λ_{max} remains the same (e.g. BLYP > PBE0 > LC-BLYP) upon varying the basis set. The extended basis sets are often recommended for the calculation of hyperpolarizabilities and excited-state properties.[92–94] Our data further corroborate this. At a minimum, the 6-31+G(d) basis set must be used in such calculations. However, it is worthwhile noting that use of diffuse functions in the calculations of the excited-state properties and hyperpolarizabilities is not always feasible for the complexes studied here.

3. Conclusions

The performance of the CAM-B3LYP, ωB97X, and LC-BLYP long-range corrected DFT methods in calculating molecular first hyperpolarizabilities and low-lying charge-transfer transitions of metal alkynyl complexes was assessed. The non-LC BLYP, B3LYP, and PBE0 functionals and the HF method were also examined. The key findings can be summarized as below:

1) For a given complex, the calculated static β value decreases in the order of BLYP > B3LYP > PBE0 > CAM-B3LYP > ωB97X > LC-BLYP > HF; long-range correction leads to a significant reduction in the calculated β. The performance of the BLYP pure functional is quite poor for the larger complexes (e.g. **5** and **6**), significantly overestimating β. In contrast, all range-separated functionals underestimate the static hyperpolarizabilities of **1**–**6**. However, most importantly, hyperpolarizability ratios between **4**, **5**, and **6** (i.e. increasing conjugation) calculated by the RS-DFT methods are in much better agreement with the experimental ratios than the conventional methods, including the hybrid functionals.

2) Calculation of frequency-dependent hyperpolarizabilities at 1064 nm by the conventional methods are significantly enhanced due to resonance effects. In contrast, the dynamic responses from CAM-B3LYP, ωB97X, and LC-BLYP are free from resonance effects because their low-lying transitions are considerably removed from the SHG wavelength, and these calculations reproduce the experimental trend for **4**–**6** (i.e. **4** < **5** < **6**).

3) The CAM-B3LYP, ωB97X, and LC-BLYP long-range corrected functionals considerably overestimate the energies of the low-energy CT transitions in **2**, **4**, and **5**. BLYP, on the other hand, significantly underestimates the excitation energies. The performance of the B3LYP and PBE0 functionals is much better than BLYP. Compared to transitions calculated using functionals lacking long-range corrections, the significantly blue-shifted low-energy CT transitions for the RS-DFT functionals account for the reduction in the calculated β values.

4) The influence of the phenylene ring orientation in the alkynyl ligand on the optical properties is significant. Specifically, the impact is much stronger for the complexes containing multiple phenyleneethylene groups. Hence, comparisons of experimental data, which is an average of conformations, with calculations on the basis of a single conformer should be made with care. However, calculations performed on the coplanar conformations yield correct trends in β, which is important for identifying potent NLO chromophores from related but less efficient compounds. Further, for these type of calculations, we recommend using a basis set with diffuse functions (at least 6-31+G(d)) for heavy elements, if feasible.

Acknowledgements

The authors gratefully acknowledge the Australian Research Council (ARC) for financial support and also access to the Australian National University supercomputer facilities of the National Computational Infrastructure.

Keywords: Density functional calculations• Nonlinear optics • Excitation energy • Organometallics • Transition metals

[1] P. N. Prasad, D. J. Williams, *Introduction to Nonlinear Optical Effects in Molecules and Polymers*, Wiley, New York, **1991**.

[2] Y. R. Shen, *The Principles of Nonlinear Optics*, Wiley, New York, **1984**.

[3] P. Günter, in *Nonlinear Opt. Eff. Mater.* (Ed.: P. Günter), Springer, New York, **2000**.

[4] G. D. Stucky, S. R. Marder, J. E. Sohn, in *Mater. Nonlinear Opt.* (Eds.: S.R. Marder, J.E. Shon, G.D. Stucky), American Chemical Society, Washington, D.C., **1991**, pp. 2–30.

[5] D. J. Williams, *Nonlinear Optical Properties of Organic and Polymeric Materials*, American Chemical Society, Washington, D.C., **1983**.

[6] S. D. Bella, *Chem. Soc. Rev.* **2001**, *30*, 355–366.

[7] H. S. Nalwa, *Appl. Organomet. Chem.* **1991**, *5*, 349–377.

[8] S. D. Bella, C. Dragonetti, M. Pizzotti, D. Roberto, F. Tessore, R. Ugo, in *Mol. Organomet. Mater. Opt.* (Eds.: H. Le Bozec, V.

Guerchais), Springer, New York, **2010**, pp. 1–55.

[9] N. J. Long, *Angew. Chemie - Int. Ed.* **1995**, *34*, 21–38.

[10] K. A. Green, M. P. Cifuentes, M. Samoc, M. G. Humphrey, *Coord. Chem. Rev.* **2011**, *255*, 2025–2038.

[11] J. P. L. Morrall, M. P. Cifuentes, M. G. Humphrey, R. Kellens, E. Robijns, I. Asselberghs, K. Clays, A. Persoons, M. Samoc, A. C. Willis, *Inorganica Chim. Acta* **2006**, *359*, 998–1005.

[12] P. V. Simpson, L. A. Watson, A. Barlow, G. Wang, M. P. Cifuentes, M. G. Humphrey, *Angew. Chemie - Int. Ed.* **2016**, *55*, 2387–2391.

[13] B. Gao, L. M. Mazur, M. Morshedi, A. Barlow, H. Wang, C. Quintana, C. Zhang, M. Samoc, M. P. Cifuentes, M. G. Humphrey, *Chem. Commun.* **2016**, *52*, 8301–8304.

[14] D. R. Kanis, M. A. Ratner, T. J. Marks, *Chem. Rev.* **1994**, *94*, 195–242.

[15] L. R. Dalton, S. J. Benight, L. E. Johnson, D. B. Knorr, I. Kosilkin, B. E. Eichinger, B. H. Robinson, A. K. Y. Jen, R. M. Overney, *Chem. Mater.* **2011**, *23*, 430–445.

[16] L. R. Dalton, P. A. Sullivan, D. H. Bale, *Chem. Rev.* **2010**, *110*, 25–55.

[17] C. E. Powell, M. G. Humphrey, *Coord. Chem. Rev.* **2004**, *248*, 725–756.

[18] B. Champagne, E. A. Perpète, D. Jacquemin, S. J. A. van Gisbergen, E.-J. Baerends, C. Soubra-Ghaoui, K. A. Robins, B. Kirtman, *J. Phys. Chem. A* **2000**, *104*, 4755–4763.

[19] D. Jacquemin, J. M. André, E. A. Perpète, *J. Chem. Phys.* **2004**, *121*, 4389–4396.

[20] D. Jacquemin, E. A. Perpète, M. Medved', G. Scalmani, M. J. Frisch, R. Kobayashi, C. Adamo, *J. Chem. Phys.* **2007**, *126*, 191108.

[21] M. de Wergifosse, B. Champagne, *J. Chem. Phys.* **2011**, *134*, 74113.

[22] L. E. Johnson, L. R. Dalton, B. H. Robinson, *Acc. Chem. Res.* **2014**, *47*, 3258–3265.

[23] J. R. Hammond, K. Kowalski, *J. Chem. Phys.* **2009**, *130*, 194108.

[24] H. Sekino, Y. Maeda, M. Kamiya, K. Hirao, *J. Chem. Phys.* **2007**, *126*, 14107.

[25] S. Nénon, B. Champagne, M. I. Spassova, *Phys. Chem. Chem. Phys.* **2014**, *16*, 7083–7088.

[26] K. Y. Suponitsky, S. Tafur, A. E. Masunov, *J. Chem. Phys.* **2008**, *129*, 44109.

[27] M. De Wergifosse, F. Wautelet, B. Champagne, R. Kishi, K. Fukuda, H. Matsui, M. Nakano, *J. Phys. Chem. A* **2013**, *117*, 4709–4715.

[28] F. Sim, S. Chin, M. Dupuis, J. E. Rice, *J Phys Chem* **1993**, *97*, 1158–1163.

[29] A. Dreuw, M. Head-Gordon, *J. Am. Chem. Soc.* **2004**, *126*, 4007–4016.

[30] D. J. Tozer, R. D. Amos, N. C. Handy, B. O. Roos, L. Serrano-ANDRES, *Mol. Phys.* **1999**, *97*, 859–868.

[31] L. Bernasconi, M. Sprik, J. Hutter, *J. Chem. Phys.* **2003**, *119*, 12417–12431.

[32] Y. Tawada, T. Tsuneda, S. Yanagisawa, T. Yanai, K. Hirao, *J. Chem. Phys.* **2004**, *120*, 8425–8433.

[33] H. Sekino, Y. Maeda, M. Kamiya, *Mol. Phys.* **2005**, *103*, 2183–2189.

[34] M. Kamiya, H. Sekino, T. Tsuneda, K. Hirao, *J. Chem. Phys.* **2005**, *122*, 234111.

[35] T. Yanai, D. P. Tew, N. C. Handy, *Chem. Phys. Lett.* **2004**, *393*, 51–57.

[36] J. Da Chai, M. Head-Gordon, *J. Chem. Phys.* **2008**, *128*, 844106.

[37] B. F. Levine, C. G. Bethea, *J. Chem. Phys.* **1975**, *63*, 2666.

[38] K. Clays, A. Persoons, *Phys. Rev. Lett.* **1991**, *66*, 2980–2983.

[39] K. Clays, A. Persoons, *Rev. Sci. Instrum.* **1992**, *63*, 3285–3289.

[40] C. Dhenaut, I. Ledoux, I. D. W. Samuel, J. Zyss, M. Bourgault, H. Le Bozec, *Nature* **1995**, *374*, 339–342.

[41] S. Brasselet, J. Zyss, *J. Opt. Soc. Am. B* **1998**, *15*, 257.

[42] W. M. Laidlaw, R. G. Denning, T. Verbiest, E. Chauchard, A. Persoons, *Naure* **1993**, *363*, 58–60.

[43] B. J. Coe, J. a. Harris, K. Clays, A. Persoons, K. Wostyn, B. S. Brunschwig, *Chem. Commun.* **2001**, *6*, 1548–1549.

[44] I. D. Morrison, R. G. Denning, W. M. Laidlaw, M. A. Stammers, *Rev. Sci. Instrum.* **1996**, *67*, 1445–1453.

[45] G. J. T. Heesink, A. G. T. Ruiter, N. F. Van Hulst, B. Bölger, *Phys. Rev. Lett.* **1993**, *71*, 999–1002.

[46] P. Kaatz, D. P. Shelton, *J Chem Phys* **1996**, *105*, 3918–3929.

[47] J. P. Morrall, G. T. Dalton, M. G. Humphrey, M. Samoc, *Adv. Organomet. Chem.* **2007**, *55*, 61–136.

[48] G. Grelaud, M. P. Cifuentes, F. Paul, M. G. Humphrey, *J. Organomet. Chem.* **2014**, *751*, 181–200.

[49] H. Zhang, M. Morshedi, M. S. Kodikara, G. J. Moxey, G. Wang, H. Wang, C. Quintana, R. Stranger, C. Zhang, M. P. Cifuentes, et al., *Chempluschem* **2016**, *81*, 613–620.

[50] E. Kulasekera, S. Petrie, R. Stranger, M. G. Humphrey, *Organometallics* **2014**, *33*, 2434–2447.

[51] H. Iikura, T. Tsuneda, T. Yanai, K. Hirao, *J. Chem. Phys.* **2001**, *115*, 3540.

[52] C. E. Powell, M. P. Cifuentes, A. M. McDonagh, S. K. Hurst, N. T. Lucas, C. D. Delfs, R. Stranger, M. G. Humphrey, S. Houbrechts, I. Asselberghs, et al., *Inorganica Chim. Acta* **2003**, *352*, 9–18.

[53] R. H. Naulty, A. M. McDonagh, I. R. Whittall, M. P. Cifuentes, M. G. Humphrey, S. Houbrechts, J. Maes, A. Persoons, G. A. Heath, D. C. . Hockless, *J. Organomet. Chem.* **1998**, *563*, 137–146.

[54] S. K. Hurst, M. P. Cifuentes, J. P. L. Morrall, N. T. Lucas, I. R. Whittall, M. G. Humphrey, I. Asselberghs, A. Persoons, M. Samoc, B. Luther-Davies, et al., *Organometallics* **2001**, *20*, 4664–4675.

[55] J. L. Oudar, *J. Chem. Phys.* **1977**, *67*, 446.

[56] J. L. Oudar, D. S. Chemla, *J. Chem. Phys.* **1977**, *66*, 2664.

[57] H. Iikura, T. Tsuneda, T. Yanai, K. Hirao, *J. Chem. Phys.* **2001**, *115*, 3540–3544.

[58] O. A. Vydrov, J. Heyd, A. V. Krukau, G. E. Scuseria, *J. Chem. Phys.* **2006**, *125*, 74106.

[59] O. A. Vydrov, G. E. Scuseria, *J. Chem. Phys.* **2006**, *125*, 234109.

[60] A. Savi, in *Recent Dev. Appl. Mod. Density Funct. Thoery* (Ed.: J.M. Seminario), Elsevier, Amsterdam, **1996**.

[61] T. Leininger, H. Stoll, H.-J. Werner, A. Savin, *Chem. Phys. Lett.* **1997**, *275*, 151–160.

[62] J. Heyd, G. E. Scuseria, M. Ernzerhof, *J. Chem. Phys.* **2003**, *118*, 8207–8215.

[63] R. Baer, D. Neuhauser, *Phys. Rev. Lett.* **2005**, *94*, 2–5.

[64] I. C. Gerber, J. G. Ángyán, *Chem. Phys. Lett.* **2005**, *415*, 100–105.

[65] Gaussian, Revision D.01, M. J. Frisch, G. W. Trucks, H. B. Schlegel,

G. E. Scuseria, M. A. Robb, J. R. Cheeseman, G. Scalmani, V. Barone, G. Petersson, A., H. Nakatsuji, et al., Gaussian, Inc., Wallingford CT, **2009**.

[66] A. D. Becke, *J. Chem. Phys.* **1993**, *98*, 5648–5652.

[67] C. Lee, W. Yang, R. G. Parr, *Phys. Rev. B* **1988**, *37*, 785–789.

[68] A. D. Becke, *Phys. Rev. A* **1988**, *38*, 3098–3100.

[69] P. J. Stephens, F. J. Devlin, C. F. Chabalowski, M. J. Frisch, *J. Phys. Chem.* **1994**, *98*, 11623–11627.

[70] C. Adamo, V. Barone, *J. Chem. Phys.* **1999**, *110*, 6158–6170.

[71] M. Diedenhofen, T. Wagener, G. Frenking, in *Comput. Organomet. Chem.* (Ed.: T.R. Cundari), **2001**, pp. 69–121.

[72] H. T. Andrae, D.; Häußermann, U.; Dolg, M.; Stoll, H.; Preuß, *Theor. Chim. Acta* **1990**, *77*, 123–141.

[73] N. M. O'Boyle, A. L. Tenderholt, K. M. Langner, *J. Comput. Chem.* **2008**, *29*, 839–845.

[74] S. R. Marder, D. N. Beratan, B. G. Tiemann, L.-T. Cheng, W. Tam, in *Org. Mater. Nonlinear Opt. II* (Eds.: R.A. Hann, D. Bloor), The Royal Society Of Chemistry, Cambridge, **1991**, pp. 165–175.

[75] A. M. Moran, D. S. Egolf, M. Blanchard-Desce, A. M. Kelley, *J. Chem. Phys.* **2002**, *116*, 2542–2555.

[76] M. P. Robalo, A. P. S. Teixeira, M. H. Garcia, M. F. Minas da Piedade, M. T. Duarte, A. R. Dias, J. Campo, W. Wenseleers, E. Goovaerts, *Eur. J. Inorg. Chem.* **2006**, *2006*, 2175–2185.

[77] M. P. Cifuentes, M. G. Humphrey, *J. Organomet. Chem.* **2004**, *689*, 3968–3981.

[78] J. Andre, J. Delhalle, *Chem. Rev.* **1991**, *91*, 843–865.

[79] H. Kurtz, D. Dudis, *Rev. Comput. Chem.* **1998**, *12*, 241–279.

[80] B. Jansik, P. Sałek, D. Jonsson, O. Vahtras, H. Agren, *J. Chem. Phys.* **2005**, *122*, 54107.

[81] E. A. Perpète, B. Champagne, D. Jacquemin, *J. Mol. Struct. THEOCHEM* **2000**, *529*, 65–71.

[82] G. J. B. Hurst, M. Dupuis, E. Clementi, *J. Chem. Phys.* **1988**, *89*, 385.

[83] I. R. Whittall, M. G. Humphrey, D. C. R. Hockless, B. W. Skelton, A. H. White, *Organometallics* **1995**, *14*, 3970–3979.

[84] I. R. Whittall, M. P. Cifuentes, M. G. Humphrey, B. Luther-Davies, M. Samoc, S. Houbrechts, A. Persoons, G. A. Heath, D. C. R. Hockless, *J. Organomet. Chem.* **1997**, *549*, 127–137.

[85] S. Houbrechts, K. Clays, A. Persoons, V. Cadierno, M. P. Gamasa, J. Gimeno, **1996**, *15*, 5266–5268.

[86] V. Cadierno, S. Conejero, M. P. Gamasa, J. Gimeno, I. Asselberghs, S. Houbrechts, K. Clays, A. Persoons, J. Borge, S. Granda-Garcia, **1999**, *18*, 582–597.

[87] B. Babgi, L. Rigamonti, M. P. Cifuentes, T. C. Corkery, M. D. Randles, T. Schwich, S. Petrie, R. Stranger, A. Teshome, I. Asselberghs, et al., *J. Am. Chem. Soc.* **2009**, *131*, 10293–10307.

[88] G. T. Dalton, M. P. Cifuentes, L. A. Watson, S. Petrle, R. Stranger, M. Samoc, M. G. Humphrey, *Inorg. Chem.* **2009**, *48*, 6534–6547.

[89] S. Marqués-González, M. Parthey, D. S. Yufit, J. A. K. Howard, M. Kaupp, P. J. Low, *Organometallics* **2014**, *33*, 4947–4963.

[90] V. W. W. Yam, K. M. C. Wong, N. Zhu, *Angew. Chem. Int - Ed.* **2003,** 12, 1400–1403

[91] H. Sahnoune, N. Gauthier, K. Green, K. Costuas, F. Paul, J. F. Halet, *Aust. J. Chem.* **2015**, *68*, 1352–1358.

[92] S. Liu, C. E. Dykstra, *J. Phys. Chem.* **1987**, *91*, 1749–1754.

[93] D. Feller, E. R. Davidson, in *Rev. Comput. Chem. Vol. 1* (Eds.: K.B. Lipkowitz, D.B. Boyd), **1990**, pp. 1–43.

[94] C. Adamo, D. Jacquemin, *Chem. Soc. Rev.* **2013**, *42*, 845–856.

Entry for the Table of Contents (Please choose one layout)

ARTICLE

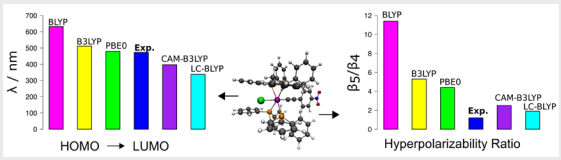

Old Vs New: A comparison between different DFT functionals, including recently introduced long-range corrected and conventional DFT methods, has been made in the calculation of first hyperpolarizabilities and excitation energies of low-lying charge transfer transitions in metal alkynyl complexes.

Mahesh S. Kodikara, Rob Stranger, Mark G. Humphrey*

Page No. – Page No.

Long-Range Corrected DFT Calculations of First Hyperpolarizabilities and Excitation Energies of Metal Alkynyl complexes